Oxygen polarity and interfacial atomic arrangement in an Mg$_x$Zn$_{1-x}$O/C-MgO/sapphire heterostructure

Oxygen polarity and interfacial atomic arrangement in an Mg$_x$Zn$_{1-x}$O/C-MgO/sapphire heterostructure

Xiang He[1], Lin Gu[1], Sandong Guo[1], Zhanglong Liu[1], Richeng Yu[1], Zengxia Mei[1,5], Xiaolong Du[1], Banggui Liu[1], Yuichi Ikuhara[2,3,4] and Xiaofeng Duan[1,5]

[1] Beijing National Laboratory for Condensed Matter Physics, Institute of Physics, Chinese Academy of Sciences, Beijing 100190, People's Republic of China
[2] WPI Advanced Institute for Materials Research, Tohoku University, Sendai 980-8577, Japan
[3] Institute of Engineering Innovation, the University of Tokyo, Tokyo 113-8656, Japan
[4] Nanostructures Research Laboratory, Japan Fine Ceramic Centre, Nagoya 456-8587, Japan

E-mail: xfduan@blem.ac.cn and zxmei@aphy.iphy.ac.cn

Abstract
Oxygen polarity and interfacial structure of an Mg$_{0.55}$Zn$_{0.45}$O/Mg$_{0.17}$Zn$_{0.83}$O/MgO/sapphire heterostructure were determined by electron energy-loss spectroscopy and aberration-corrected scanning transmission electron microscopy. It was found that O-polarity occurs by an uncommon mechanism in the Mg$_x$Zn$_{1-x}$O film with a 0.5 nm-thick compressively strained rocksalt MgO buffer; and that the ∼18% lattice mismatch between Mg$_{0.17}$Zn$_{0.83}$O and sapphire is mostly accommodated by misfit dislocations at the Mg$_{0.17}$Zn$_{0.83}$O/MgO interface. Density functional theory calculations indicate that the MgO buffer strongly tends to manifest a rocksalt structure rather than wurtzite. Zn substitution of the topmost Mg atoms in the MgO buffer is likely to induce such O-polarity.

(Some figures may appear in colour only in the online journal)

ZnO has attracted considerable attention for potential applications in optoelectronic devices in the ultraviolet (UV) region [1, 2]. It has a stable hexagonal wurtzite structure and a direct band gap of 3.3 eV. Alloying wurtzite ZnO with rocksalt MgO ($E_{gap} = 7.8$ eV) allows the band gap to be controlled between 3.3 and 7.8 eV. Thus, wurtzite Mg$_x$Zn$_{1-x}$O films with tunable band gaps are promising candidates for UV light emitters [3], solar-blind UV detectors and other optoelectronic UV-range devices relying on heterostructure functionalities [4].

Till now, Mg$_x$Zn$_{1-x}$O epitaxial films have been mostly fabricated on widely used low-cost c-sapphire substrates. However, due to the large lattice and thermal mismatch, Mg$_x$Zn$_{1-x}$O films grown directly on sapphire substrates

have rough surface morphology and poor crystal quality [5]. Therefore, an ultrathin MgO buffer layer has been used by researchers to obtain high-quality Mg$_x$Zn$_{1-x}$O films on sapphire substrates. Photodetectors based on this material have been realized with a sharp solar-blind cutoff [6]. It is obvious that an Mg$_x$Zn$_{1-x}$O/MgO/sapphire heterostructure is significant for potential applications in deep UV optoelectronic devices.

In recent years, many reports on ZnO/MgO/sapphire interface structures have emerged [7–12], and researchers came to believe that an ultrathin (<1 nm) MgO buffer deposited on c-sapphire has an O-polar wurtzite structure, which induces O-polar ZnO (or Mg$_x$Zn$_{1-x}$O) deposition, whereas thicker (>2 nm) MgO with a rocksalt structure induces Zn-polar ZnO deposition. Unfortunately, so far, experiments with reflection high-energy electron diffraction (RHEED) or normal

---

[5] Authors to whom any correspondence should be addressed.

1

high-resolution transmission electron microscopy (HRTEM) have failed to reveal the atomic structure at the interface. Here we report the atomic arrangement of an $Mg_xZn_{1-x}O$/ultrathin MgO/sapphire heterostructure observed by a sub-angstrom Cs-corrected scanning transmission electron microscope, which is essential for understanding the ultrafine interface structure and its role in the polarity selection mechanism of high-quality $Mg_xZn_{1-x}O$ epilayers. Density functional theory (DFT) calculations were also performed to confirm our results.

The heterostructure was deposited on a sapphire (0 0 0 1) substrate by rf-plasma-assisted molecular beam epitaxy (rf-MBE) with a base pressure of $\sim 1 \times 10^{-10}$ mbar [13]. Elemental Zn (7N) and Mg (5N) evaporated by Knudsen cells (CreaTech) and oxygen radicals (5N5) generated by an rf-plasma system (SVTA) were used as sources for the growth. Sapphire substrates were thermally cleaned at 750 °C for 30 min, and then exposed to an oxygen plasma (350 W/2.5 sccm) at 250 °C to obtain a uniform oxygen-terminated surface [14]. After that, an ultrathin MgO buffer layer (thinner than 1 nm) was carefully prepared at 500 °C. About 30 nm thick quasi-homo low-Mg-content $Mg_{0.17}Zn_{0.83}O$ buffer was subsequently deposited at 450 °C. Finally, a high-Mg-content $Mg_{0.55}Zn_{0.45}O$ epilayer was grown at 450 °C. The growth pressure of $Mg_xZn_{1-x}O$ was kept at 4.5×10^{-5} mbar. The film thickness was determined to be 200 nm measured by a Dektak 8 surface profiler (Veeco). It should be noted that the deposition temperature of MgO was optimized between 400 and 600 °C, which was found to have no influence on the structure of this ultrathin layer. Once the thickness of MgO increases even a little, however, strain relaxation and structure transition occur, indicated by an evolution of dotted RHEED patterns. In that case, phase separation tends to occur in high-Mg-content $Mg_{0.55}Zn_{0.45}O$ growth. This clearly demonstrates the strong dependence of $Mg_{0.55}Zn_{0.45}O$ growth on the MgO buffer thickness, in particular on the highly strained cubic structure obtained in later scanning transmission electron microscopy (STEM) experiments.

Crystallographic properties of the $Mg_{0.55}Zn_{0.45}O$ sample were studied by x-ray diffraction (XRD) and high-resolution XRD using a light source from synchrotron radiation. The θ–2θ scan results indicate that the film consists solely of the wurtzite phase [15]. The full-width at half-maximum (FWHM) of the (0 0 2) rocking curve is 0.23°, suggesting the high crystal quality of the $Mg_{0.55}Zn_{0.45}O$ film. The 40 K photoluminescence (PL) peak energy and FWHM of the PL emission peak are found to be 4.345 eV and 214 meV, respectively [16]. The sample is n-type with very high resistivity, which is quite reasonable considering the high Mg content.

The [1 1 −2 0] $Mg_xZn_{1-x}O$ cross-sectional TEM samples were mechanically thinned down to 10 μm, and subsequently thinned to electron transparency by Ar ion milling. The selected-area electron diffraction (SAED), dark-field imaging and electron energy-loss spectroscopy (EELS) were carried out in a Tecnai F20 ST transmission electron microscope operated at 200 kV equipped with a Gatan filter system. The aberration-corrected STEM high-angle angular-dark-field (HAADF) and angular-bright-field (ABF) images were acquired using a JEOL
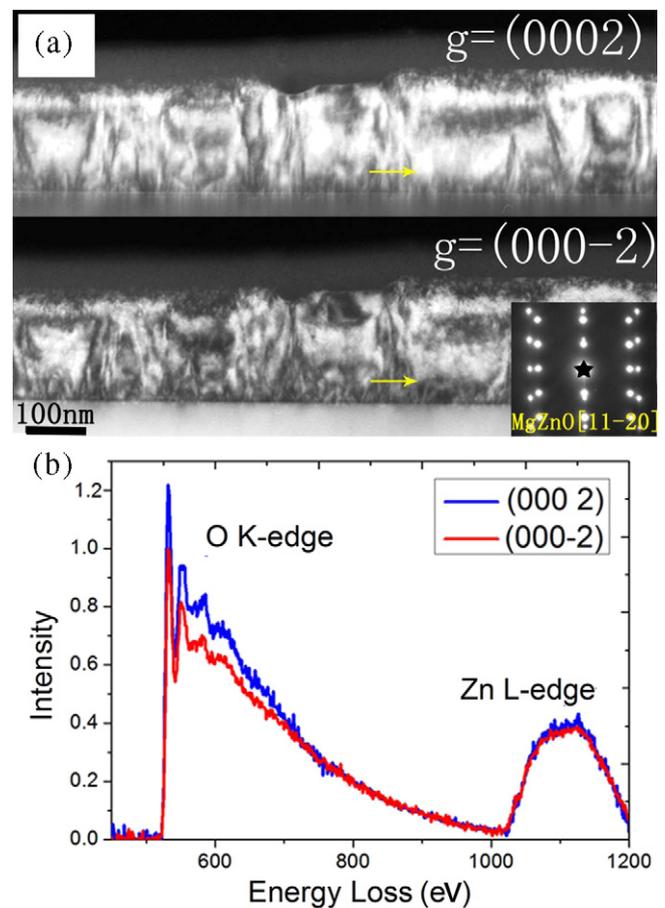
Figure 1. (*a*) Two-beam dark-field images of the $Mg_xZn_{1-x}O$/MgO/sapphire heterostructure near the $Mg_xZn_{1-x}O$ [1 1 −2 0] axis with $g = (0 0 0 2)$ and $g = (0 0 0 \text{-}2)$, respectively. The yellow arrows indicate the interface between the $Mg_{0.55}Zn_{0.45}O$ layer and the $Mg_{0.17}Zn_{0.83}O$ layer. The inset shows the SAED pattern of the heterostructure in the $Mg_xZn_{1-x}O$ [1 1 −2 0] direction. (*b*) EELS of the $Mg_xZn_{1-x}O$ film acquired at (0 0 0 2) and (0 0 0 −2) Bragg conditions with the background subtracted.

2100F (JEOL, Tokyo, Japan) electron microscope equipped with a probe corrector. The convergent semiangle was set to 20 mrad, and the detection semiangles of HAADF and ABF were $60 < \theta < 150$ mrad and $10 < \theta < 20$ mrad, respectively.

Figure 1(*a*) presents the $Mg_xZn_{1-x}O$ (0 0 0 2) and (0 0 0 −2) dark-field images of the $Mg_xZn_{1-x}O$/MgO/sapphire heterostructure. The heterostructure consists of three sections: sapphire substrate, 30 nm thick $Mg_{0.17}Zn_{0.83}O$ quasi-homo buffer layer and 200 nm thick $Mg_{0.55}Zn_{0.45}O$ film. The MgO buffer is too thin to be visible in the dark-field images. The inset of figure 1(*a*) shows the traditional SAED pattern of the heterostructure in the $Mg_xZn_{1-x}O$ [1 1 −2 0] direction. By comparison of the (0 0 0 2) and (0 0 0 −2) dark-field images, it is confirmed that no inversion domain exists in the $Mg_xZn_{1-x}O$ film, implying that the $Mg_xZn_{1-x}O$ epilayer is of single polarity. EELS was performed to deduce the polarity of the $Mg_xZn_{1-x}O$ film [17]. Figure 1(*b*) shows the background-subtracted O K-edge obtained at $Mg_xZn_{1-x}O$ (0 0 0 2) and (0 0 0 −2) Bragg conditions, respectively. The O K-edge is more intense at (0 0 0 2) than at (0 0 0 −2), which reveals the uniform O-polarity of the $Mg_xZn_{1-x}O$ film.
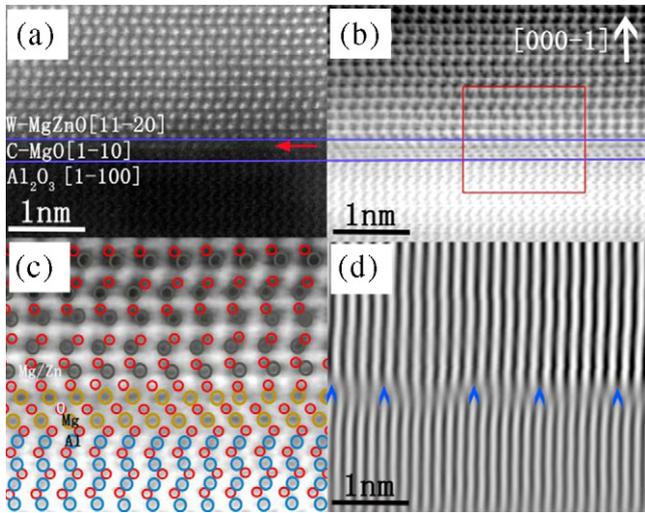
Figure 2. (*a*) HAADF and (*b*) ABF STEM images of the $Mg_{0.17}Zn_{0.83}O/MgO/sapphire$ heterostructure in the $Mg_{0.17}Zn_{0.83}O$ [1 1 −2 0] direction. Red arrow in (*a*) indicates the topmost Mg atom layer in MgO, which is brighter than the lower layer. (*c*) Magnified image of the boxed area in (*b*). Different elements are marked by different colours: red, O; blue, Al; yellow, Mg; gray, $Mg_{0.17}Zn_{0.83}$ mixed atoms. (*d*) Fourier-filtered image of the ABF STEM image (*b*). Blue arrows indicate where the misfit dislocations are located.

Figures 2(*a*) and (*b*) present simultaneously acquired HAADF and ABF STEM images of the heterostructure in the $Mg_{0.17}Zn_{0.83}O$ [1 1 −2 0] direction. Since the contrast of an HAADF STEM micrograph is atomic number dependent and heavier elements produce a brighter contrast, the $Mg_{0.17}Zn_{0.83}O$ film has a much brighter contrast than that of the MgO buffer and sapphire substrate. However, the ABF STEM technique is more sensitive for light elements, with the interfacial structure clearly shown in figure 2(*b*). Note that the two interfaces of the $Mg_{0.17}Zn_{0.83}O/MgO/sapphire$ heterostructure are indicated by straight blue lines in both figures 2(*a*) and (*b*).

Figure 2(*c*) shows an enlarged micrograph from the boxed area in figure 2(*b*). Atoms from different elements in figure 2(*c*) are marked by different coloured circles; and the $Mg_{0.17}Zn_{0.83}O/MgO/sapphire$ interfaces can be clearly viewed. Note that the sapphire has a zigzag projective structure in the [1 −1 0 0] direction and the O atoms lie on the inflections of the zigzag structure. It can be deduced that the surface of the sapphire (0 0 0 1) slab's edge in figure 2(*c*) is coated with an O atom layer, which provides solid confirmation of O termination by an oxygen plasma pretreatment [7, 14]. The MgO buffer with two MgO monolayers deposited on the O-terminated sapphire substrate in figure 2(*c*) displays a face-centred cubic (fcc) arrangement, which unquestionably confirms the rocksalt structure of our ultrathin MgO buffer. In figure 2(*a*) the upper Mg atom layer marked by a red arrow in the MgO buffer is brighter than the lower Mg atom layer, confirming that some of the topmost Mg atoms in the MgO buffer were replaced by Zn atoms. From figure 2(*b*), no misfit dislocation is found at the interface of the MgO buffer and the sapphire substrate, which indicates that the MgO buffer is not relaxed but compressively strained since there is

about 8% misfit between bulk MgO and sapphire. Thus, the presence of the MgO buffer does not reduce the lattice misfit (about 18%) between $Mg_{0.17}Zn_{0.83}O$ and sapphire. Figure 2(*c*) also shows that the misfit dislocations due to the large lattice mismatch start at the interface between C-MgO and W-$Mg_{0.17}Zn_{0.83}O$ layers. To analyse the misfit dislocations at the interface, a Fourier-filtered image of figure 2(*b*) is shown in figure 2(*d*). Blue arrows in figure 2(*d*) indicate where the misfit dislocations are located. From this figure, we found the so-called domain epitaxy [18] a 5 : 6 matching of major planes across the $Mg_{0.17}Zn_{0.83}O/MgO$ interface. It is clear that the very large lattice misfit between the $Mg_{0.17}Zn_{0.83}O$ film and the sapphire substrate is mostly accommodated by misfit dislocations at the $Mg_{0.17}Zn_{0.83}O/MgO$ interface; thus a high-quality epitaxial $Mg_xZn_{1-x}O$ film can be obtained. Considering that the Al–O bond in sapphire and the Mg–O bond in C-MgO are much stronger than the Zn–O in the W-$Mg_{0.17}Zn_{0.83}O$ film, and the MgO buffer here is only 0.5 nm thick, it makes sense that the misfit dislocations lie at the $Mg_{0.17}Zn_{0.83}O/MgO$ interface. Since the Zn and O atoms of W-$Mg_{0.17}Zn_{0.83}O$ can be identified in the ABF STEM image (figure 2(*c*)), we can determine the polarity of W-$Mg_{0.17}Zn_{0.83}O$ directly by the atomic arrangement. The O-polarity of the W-$Mg_xZn_{1-x}O$ film shown in figure 2(*c*) agrees well with the EELS result (figure 1(*b*)). The orientation relationship of the heterostructure is verified to be $Mg_xZn_{1-x}O(0 0 0 −1)//MgO(1 1 1)//sapphire(0 0 0 1)$ and $Mg_xZn_{1-x}O[1 1 −2 0]//MgO[1 −1 0]//sapphire[1 −1 0 0]$.

The above findings about rocksalt structured MgO plainly differ from former reports in which researchers concluded that the MgO buffer deposited on O-terminated sapphire has an O-polar wurtzite structure for thickness lower than 1 nm. To confirm our results by theory, DFT calculations were performed using the full-potential linearized augmented-plane wave method within the WIEN2k package [19]. The generalized gradient approximation (GGA) was used for the exchange-correlation potential [20]. We used a $4 \times 4 \times 1$ Monkhorst–Pack mesh in the first Brillouin zone, made the harmonic expansion up to $l_{max} = 10$ in atomic spheres, and set $R_{mt} \times K_{max}$ to 7.0. Two possible models, C-MgO and O-polar W-MgO, for the four-layer MgO buffer deposited on O-terminated 12-layer sapphire with an additional vacuum layer 1 nm thick were constructed, respectively. We optimize the internal position parameters of two of the layers of Al_2O_3 and all four layers of MgO near the interface with a force standard of 4 mRy/a.u. The self-consistent calculations are considered to have converged only when the integration of absolute charge-density difference per formula unit between the successive loops is less than $0.0001|e|$, where e is the electron charge. The energy calculations indicate that the four atomic layers of MgO deposited on sapphire tend towards a rocksalt structure rather than wurtzite by saving 0.91 eV per chemical formula unit (MgO) in total energy. The large energy difference indicates that the MgO buffer could hardly assume a wurtzite structure during the growth process and the rocksalt MgO is the stabler structure, which agrees well with our STEM ABF experiments. Based on the calculated stable model, figure 3(*a*) presents a schematic plot of the atomic structure

J. Phys. D: Appl. Phys. **46** (2013) 145303

X He *et al*
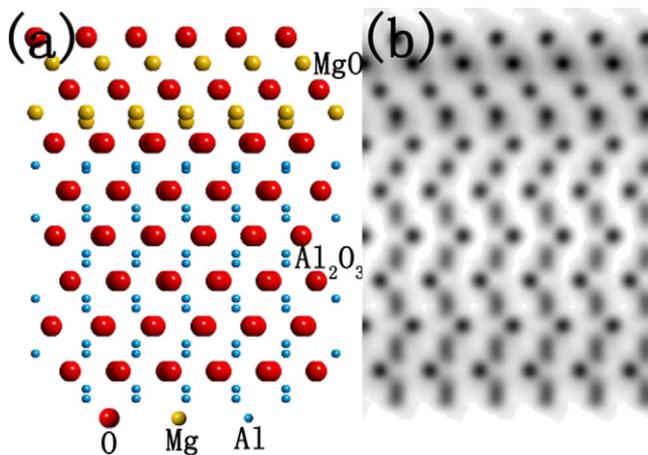
Figure 3. (*a*) Schematic plot and (*b*) simulated STEM ABF image of the calculated stable atomic structure of the MgO/sapphire interface in the sapphire [1 −1 0 0] direction.

Figure 4. Schematic plot of the atomic arrangement of wurtzite $Mg_xZn_{1-x}O$ deposited on rocksalt MgO buffer (*a*) without and (*b*) with Zn atoms substituted for some of the topmost Mg atoms in the MgO buffer.

of the MgO/sapphire interface in the [1 −1 0 0] direction of sapphire. Note that the Mg atoms immediately adjacent to the sapphire substrate have divergent Z coordinates like the Al atoms in sapphire in figure 3(*a*). This means the MgO tends to duplicate the sapphire structure at the beginning of deposition. A simulated STEM ABF image of figure 3(*a*) in the [1 −1 0 0] direction of sapphire is shown in figure 3(*b*), which is very consistent with our experimental ABF image in figure 2(*b*).

In addition, we found that the O-polar $Mg_xZn_{1-x}O$ deposited on rocksalt MgO is obviously different from previous reports in which researchers proposed that the coordination number of the O atoms at the ZnO/MgO interface determines the polarity of the wurtzite ZnO film and that the rocksalt MgO induces the Zn-polar ZnO (or $Mg_xZn_{1-x}O$) deposition. When $Mg_xZn_{1-x}O$ is directly deposited on the pure rocksalt MgO buffer, the topmost O atoms of the rocksalt MgO buffer have six coordination bonds, three pointing downwards and three upwards, whereas Zn atoms have four coordination bonds, three linking with the three O atoms underneath and one dangling bond pointing upwards along the *c*-axis. This would define a Zn-polar $Mg_xZn_{1-x}O$ deposition (figure 4(*a*)). But in our view, the topmost Mg atoms in the rocksalt MgO buffer are partially replaced by Zn atoms, which influences the coordination numbers of the subsequently deposited O atoms at the $Mg_xZn_{1-x}O$/MgO interface. Provided sufficient Mg atoms are replaced by Zn atoms in MgO, the topmost O atoms in rocksalt MgO will have four coordination bonds instead of six, three downwards and one upwards. Then, subsequently deposited Zn atoms will each have one downward bond linked with an O atom and three upward dangling bonds, which forms the O-polar surface shown in figure 4(*b*). We believe that Zn substitution for some of the topmost Mg atoms in the rocksalt MgO buffer leads to the O-polar $Mg_xZn_{1-x}O$ deposition.

In conclusion, a single O-polar W-$Mg_xZn_{1-x}O$/C-MgO/sapphire heterostructure was obtained by rf-MBE. The interface structure was clearly observed by Cs-corrected STEM HAADF and ABF experiments at the atomic level. The 0.5 nm thick MgO buffer layer is proved to have a compressively strained rocksalt structure and the ∼18% lattice mismatch between the $Mg_xZn_{1-x}O$ film and the sapphire substrate is mostly accommodated by misfit dislocations at the $Mg_xZn_{1-x}O$/MgO interface. DFT calculations also confirm the rocksalt structure of MgO deposited on the sapphire substrate. We believe that the unusual O-polar $Mg_xZn_{1-x}O$ deposited on rocksalt MgO is a consequence of Zn substitution for some of the topmost Mg atoms in the MgO layer. This finding is important for polarity control in polar epilayer growth by single atomic layer management.
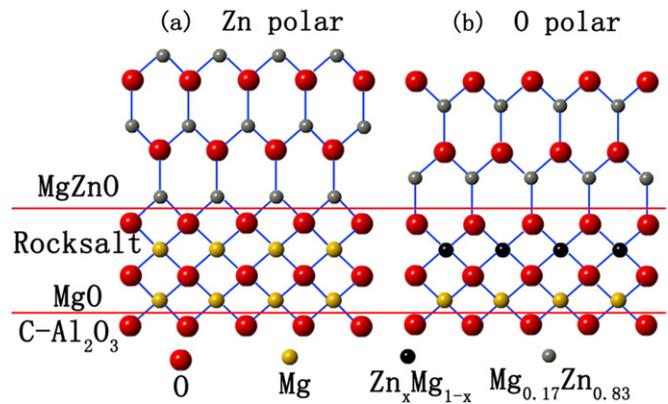
Acknowledgments

References

[1] Bagnall D M, Chen Y F, Zhu Z, Yao T, Koyama S, Shen M Y and Goto T 1997 *Appl. Phys. Lett.* **70** 2230
[2] Tang Z K, Wong G K L, Yu P, Kawasaki M, Ohtomo A, Koinuma H and Segawa Y 1998 *Appl. Phys. Lett.* **72** 3270
[3] Ohtomo A, Kawasaki M, Ohkubo I, Koinuma H, Yasuda T and Segawa Y 1999 *Appl. Phys. Lett.* **75** 980
[4] Tsukazaki A, Ohtomo A, Kita T, Ohno Y, Ohno H and Kawasaki M 2007 *Science* **315** 1388
[5] Vispute R D *et al* 1997 *Appl. Phys. Lett.* **70** 2735
[6] Hou Y N, Mei Z X, Liu Z L, Zhang T C and Du X L 2011 *Appl. Phys. Lett.* **98** 103506
[7] Chen Y F, Ko H J, Hong S K and Yao T 2000 *Appl. Phys. Lett.* **76** 559
[8] Chen Y F, Hong S K, Ko H J, Kirshner V, Wenisch H, Yao T, Inaba K and Segawa Y 2001 *Appl. Phys. Lett.* **78** 3352
[9] Yuan H T *et al* 2007 *Chin. Phys. Lett.* **24** 2408
[10] Wu X F, Huang B W, Zhan H H and Kang J Y 2011 *J. Cryst. Growth* **318** 519
[11] Kato H, Miyamoto K, Sano M and Yao T 2004 *Appl. Phys. Lett.* **84** 4562

J. Phys. D: Appl. Phys. **46** (2013) 145303

X He *et al*

[12] Minegishi T, Yoo J H, Suzuki H, Vashaei Z, Inaba K, Shim K and Yao T 2005 *J. Vac. Sci. Technol.* B **23** 1286

[13] Liu Z L, Mei Z X, Zhang T C, Liu Y P, Guo Y, Du X L, Hallen A, Zhu J J and Kuznetsov A Y 2009 *J. Cryst. Growth* **311** 4356

[14] Mei Z X, Wang Y, Du X L, Ying M J, Zeng Z Q, Zheng H, Jia J F, Xue Q K and Zhang Z 2004 *J. Appl. Phys.* **96** 7108

[15] Du X L, Mei Z X, Liu Z L, Guo Y, Zhang T C, Hou Y N, Zhang Z, Xue Q K and Kuznetsov A Y 2009 *Adv. Mater.* **21** 4625

[16] Liu Z L, Mei Z X, Wang R, Zhao J M, Liang H L, Guo Y, Kuznetsov A Y and Du X L 2010 *J. Phys. D: Appl. Phys.* **43** 285402

[17] Kong X, Hu G Q, Duan X F, Lu Y and Liu X L 2002 *Appl. Phys. Lett.* **81** 1990

[18] Narayan J and Larson B C 2003 *J. Appl. Phys.* **93** 278

[19] Blaha P, Schwarz K, Madsen G K H, Kvasnicka D and Luitz J 2001 *WIEN2k* ed K Schwarz (Vienna: Technical University)

[20] Perdew J P, Burke K and Ernzerhof M 1996 *Phys. Rev. Lett.* **77** 3865